DOI 10.1007/s10812-015-0196-7
Journal of Applied Spectroscopy, Vol. 82, No. 5, November, 2015 (Russian Original Vol. 82, No. 5, September–October, 2015)

OPTICAL STUDIES OF POLY(9,9-DI-(2-ETHYLHEXYL)-9H-FLUORENE-2,7-VINYLENE) AND ITS NANOCOMPOSITES

S. Layek,[a] M. Ghosh,[a] K. Siddarth Reddy,[a] S. Senapati,[b] P. Maiti,[b] and S. Sinha[a*]

UDC 535.372;620.3

Steady state and time-resolved spectroscopic measurements are carried out to understand the fluorescent optical properties of the conjugated polymer poly(9,9-di-(2-ethylhexyl)-9H-fluorene-2,7-vinylene) (PFV) in liquid phase and solid phase. Quite significant color tuning is observed in the fluorescence emission of PFV in the blue side of the spectra in the solid phase, especially in powder form, when the polymer is doped with 30B nanoclay (organically modified Montmorillonite) and graphene nanoparticles. Interestingly, the average fluorescence lifetime of PFV-graphene nanocomposite in thin film is found to be much higher (8.1 ns) compared to that for PFV only in thin film (3 ns). These novel nanocomposites may have potential applications in polymer optoelectronics industry.

Keywords: *poly(9,9-di-(2-ethylhexyl)-9H-fluorene-2,7-vinylene), nanoclay, graphene, nanocomposite, color tuning.*

Introduction. Fluorescent conjugated polymers are presently the focus of extreme academic and industrial interest. The discovery of the semiconducting properties of conjugated polymers in 1977 by Heeger, MacDiarmid and Shirakawa started a new era in the field of polymer research [1]. The research on conjugated polymers became even more important after 1990, when Burroughes and co-workers discovered that fluorescent conjugated polymers can exhibit emission upon electrical excitation [2]. Fluorescent conjugated polymers are a novel class of materials combining the optical and electrical properties of semiconductors with the processing advantages and mechanical properties of plastics. When functionalized with flexible side groups, these materials become soluble in many commonly used organic solvents and can be easily solution processed at room temperature into uniform, large area and optical-quality thin films.

A promising area of interest in the field of polymer optoelectronic devices is polymer nanocomposites [3, 4]. Polymer nanocomposites are a special class of materials consisting of a polymer matrix and nanoscale (dimensions of the order of 1–100 nm) inorganic or organic particles as filler. The use of nanoparticles may lead to improvements and major modifications in the mechanical, optical, electrical properties and stability of the polymer optoelectronic devices. For this purpose, various types of nanofillers like carbon nanotubes [5–7], layered double hydroxides [8], organically modified nanoclays [9–11] and recently graphene [12] have received considerable attention. However, till date, only a few reports are available on the modifications of photoluminescence properties of the fluorescent conjugated polymers in presence of nanoparticles [13–16]. In the present work, optical properties of the fluorescent conjugated polymer poly(9,9-di-(2-ethylhexyl)-9H-fluorene-2,7-vinylene) (PFV) in solution and thin film (using toluene as solvent) as well as in powder form are investigated by using steady state and time-resolved spectroscopic techniques. Also, we discuss the possibility and extent of color tuning in the fluorescence emission of PFV, especially in thin film and powder form, in presence of doped nanoparticles viz., 30B nanoclay and graphene. The time-resolved measurements reveal certain interesting features on the optical properties of PFV nanocomposites. It is to be mentioned that this is the first attempt, to the best of our knowledge, to gain more insights on the optical properties of polymer nanocomposites by time-resolved measurements (of the order of picoseconds-nanoseconds).

Nanoclays are a form of high purity aluminium silicate mineral derived from Montmorillonite (MMT), which have a disc or plate type structure and the layers are about 1 nm thick with plate diameter 100–500 nm. In order to achieve good

[*]To whom correspondence should be addressed.

[a]Integrated Science Education and Research Center, Siksha-Bhavana, Visva-Bharati, Santiniketan 731 235, India; e-mail: subratasinha67@rediffmail.com; [b]School of Materials Science and Technology, Indian Institute of Technology, Banaras Hindu University, Varanasi 221 005, India. Abstract of article is published in Zhurnal Prikladnoi Spektroskopii, Vol. 82, No. 5, p. 805, September–October, 2015.

intercalation and exfoliation, MMT nanoclays are treated with an organic modifier, methyl tallow (tallow is a mixture of C16 and C18 long chain alkenes) *bis*-hydroxyethyl quaternary ammonium salt. Such organically modified MMT nanoclays are often termed as 30B nanoclay [10]. Again, the unique electronic properties of graphene can be exploited in the development of better polymer optoelectronic devices [17]. Graphene, found experimentally only recently [18, 19], is a flat monolayer of carbon atoms tightly packed into a two-dimensional (2D) honeycomb lattice and is a basic building block for all graphitic materials of various dimensions, e.g., 0D fullerene, 1D nanotube and 3D graphite.

Experimental Procedure. The polymer PFV was used as supplied by Sigma-Aldrich. The weight-average molecular weight and polydispersity of PFV are 34,000 g/mol and 2.3, respectively. The solvent toluene of spectroscopic grade was purchased from Sigma-Aldrich and was tested before use to check the absence of any impurity emission in the wavelength region studied. For this, steady state measurements were carried out in the emission mode with toluene kept in the sample cuvette and exciting toluene at 371 and 405 nm (wavelengths used for the steady state and time-resolved emission measurements of the samples, respectively). However, no emission was detected from toluene (measured up to 900 nm). The organically modified clay, Cloisite 30B [*bis*(hydroxyethyl)methyl tallow ammonium ion exchanged montmorillonite], Southern Clay Products Inc. (Gonzales, TX), was used as the nanofiller. Graphene was purchased from Redex Technologies Private Ltd., Noida, India. Graphene (nanoflakes of graphite) was prepared by using chemical vapor deposition (CVD) method. The graphene (purity 95% by weight, specific gravity 2 gm/cc) consists of a few sheets (average area of 10,000 nm^2) with an overall thickness of approximately 3–10 nm.

The organically modified nanoclay and graphene were dispersed separately in chloroform by sonication (ultrasonicator power 1500 watt, frequency 33±3 kHz) for 15 minutes. The nanocomosites of PFV were prepared through solution route by dissolving PFV in the dispersion of 30B and graphene in chloroform separately. The solution was stirred for 6 hours at 45^{o}C to ensure homogeneous mixing, followed by evaporation of the solvent at 55^{o}C. The nanocomposites were then dried under vacuum for 24 hours. In the formation of the composites, 5% (by weight) of 30B nanoclay and graphene were used separately.

FTIR technique was applied to detect the functional groups and to understand the nature of interaction between PFV and 30B as well as graphene. FTIR was performed in the transmittance mode from 400–4000 cm^{-1} at 297 K on a Thermo Scientific FTIR (NICOLET-6700) with a resolution of 2 cm^{-1} using the KBr pellet technique. Thermal stability was examined from thermogravimetric analysis (TGA) by using a thermogravimetric analyzer (TGA, Mettler-Toledo). Data were collected in the temperature range 30–650 ^{o}C at a heating rate of 20 ^{o}C/min in nitrogen atmosphere. Thin films of the samples (using toluene as solvent) were spin coated at 2000 rpm for 30 s on glass slides by using a spin coating unit (Model SCU-2007). The steady state electronic absorption spectra of the samples were recorded by means of a JASCO V-650 absorption spectrophotometer. A rectangular quartz cuvette of 1 cm path length was used for measurements of the absorption spectra of the samples in toluene solution. Steady state fluorescence spectra of the samples were recorded by a JASCO FP-6500 fluorescence spectrometer. Emission was detected at right angles to the direction of excitation light for measurements of the emission spectra of the samples in toluene solution in order to avoid stray light. However, front-face geometry was used for measurements of the emission spectra of the samples in thin film and powder form.

The time-resolved fluorescence measurements were carried out by using a time correlated single photon counting (TCSPC) spectrometer from IBH (UK). The sample was excited with 405 nm light from a diode laser with 1 MHz repetition rate. A PMT based detector (TBX4, IBH) was used for detection of the emitted photons through a monochromator. The instrument response of the TCSPC set-up was measured by collecting the scattered light from a TiO_2 suspension in water. The instrument response function thus measured was ~200 ps. The decays were analyzed using IBH DAS-6 analysis software. The reduced χ^2, Durbin–Watson (DW) parameter, and residuals were used to judge the goodness of the fit. Emission was detected at right angles to the direction of excitation light for measurements of the fluorescence lifetime of the samples in toluene solution in order to avoid stray light. However, front-face geometry was used for measurements of the fluorescence lifetime of the samples in thin film. Unfortunately, the fluorescence lifetime of the samples in powder form could not be measured by using front-face geometry due to very low counts.

Results and Discussion. *Meterial characterization*. Figure 1 shows the FTIR spectra of PFV, PFV–30B nanocomposite and PFV–graphene nanocomposite. The vinyl C=C stretching frequency is observed at 1633 cm^{-1} for pure PFV. This peak has been shifted to 1610 cm^{-1} for PFV–30B composite and 1625 cm^{-1} for PFV–graphene composite, showing good interactions between PFV and organically modified nanoparticles. Further, 30B nanoclay interacts strongly with PFV as compared to graphene [7]. The aromatic C=C stretching is observed at 1463 cm^{-1} for pure PFV, which remains unaffected in composites. It is obvious that interaction between the π cloud from olefinic and hydroxyl groups present in organic modification in 30B nanoclay is more prominent than the π cloud present in aromatic ring presumably due to steric hindrance

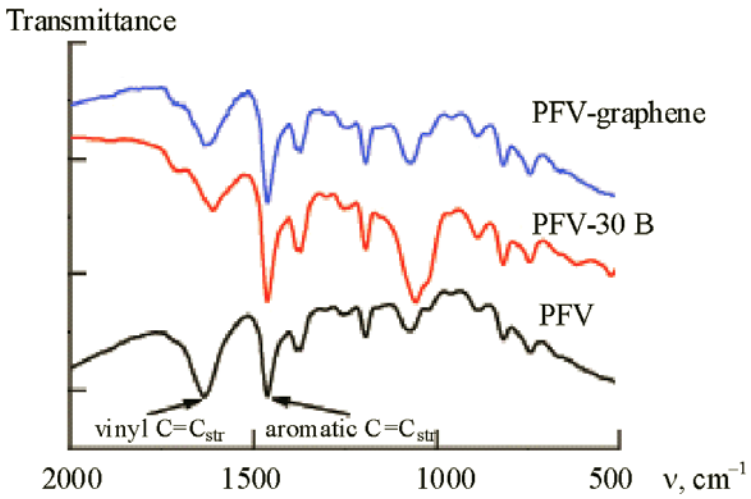

Fig. 1. FTIR spectra of PFV, PFV–30B nanocomposite and PFV–graphene nanocomposite.

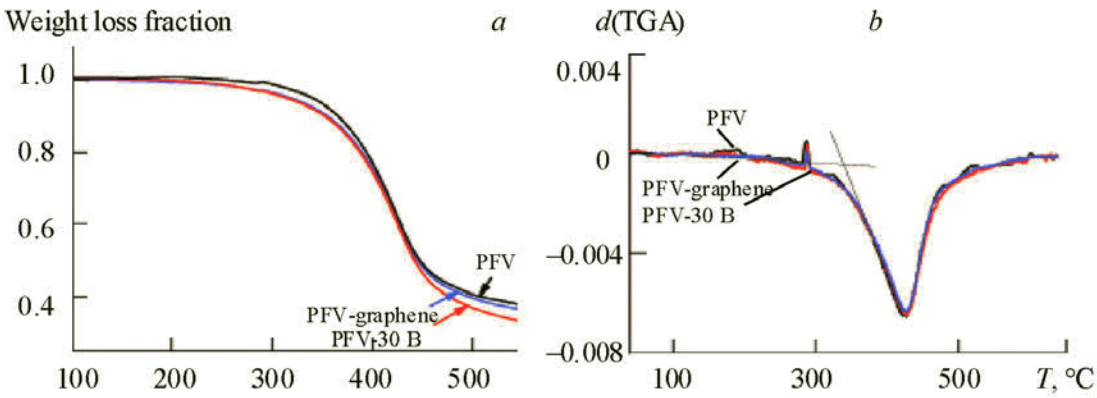

Fig. 2. TGA (a) and *d*(TGA) curves of PFV, PFV–30B nanocomposite and PFV–graphene nanocomposite (b).

arising from the bulky long chain alkyl group attached in between aromatic rings. However, FTIR spectra indicate that the interaction (primarily dipolar in nature) arises from the π cloud of the vinyl group and aromatic ring of PFV with the -OH groups of 30B in PFV–30B nanocomposite and through the π cloud of graphene in PFV–graphene nanocomposite.

The TGA curves of PFV, PFV–30B nanocomposite and PFV–graphene nanocomposite are shown in Fig. 2a. It is obvious from the figure that the degradation of the composites occurs at slightly lower temperature as compared to pure PFV. But, there is not much difference in degradation temperature of composites with respect to pure PFV, indicating good thermal stability of the composites suitable for their use at higher temperature. The derivative curves of the TGA pattern of all the samples (Fig. 2b) show similar degradation behavior of the composites with respect to pure PFV. The maximum degradation temperature is around 425^{o}C, while the onset of degradation temperature is around 340^{o}C for all the samples. It is to be mentioned that the small peak in Fig. 2b at a temperature slightly below 300^{o}C is basically a fluctuation and does not imply any specific value/meaning.

Steady-state absorption and emission spectra in solution. Figure 3a shows the normalized steady-state absorption and emission spectra of PFV in toluene solution at 297 K. The absorption spectra consist of vibrational peak energy positions at 284, 299 nm (shoulder type), 311, 371 nm and can be attributed to π,π^* transition of the conjugated backbone of the polymer. The fluorescence emission with peak intensity at 455 nm is due to radiative transition of PFV from the first excited singlet state (S_1) to the ground singlet state (S_0). The shape and peak energy position of the emission spectra are found to be independent of the excitation wavelength. Moreover, no appreciable changes are observed in the absorption as well as

emission spectra of PFV–30B and PFV–graphene nanocomposites in toluene solution compared to the corresponding spectra of PFV in toluene solution. Obviously, the interactions between the parent polymer PFV and doped nanoparticles (30B or grapheme) are insignificant in solution phase. As the polymer is solvated, it has no possibility to interact with the nanoclay or graphene in solution phase.

Steady state absorption and emission spectra in thin film. Figure 3a shows the normalized steady state absorption spectra of PFV in thin film at 297 K. The absorption spectra consist of three vibrational peaks at energy positions 300, 311, and 371 nm. Thus, the sharp peak at 284 nm observed in the absorption spectra of PFV in toluene solution is absent in the absorption spectra of PFV in thin film. However, apart from this peak, all the other three vibrational peak positions remain unchanged in the absorption spectra of PFV in solution and thin film. This seemingly indicates that the nature of the absorption band at 284 nm (observed in dilute solution only) is somewhat different from that of the absorption bands at the other three energy positions (observed in both solution and thin film). This feature is presently being investigated in detail in our laboratory and will be reported later. It is to be noted that no significant changes are observed in the absorption spectra of PFV–30B nanocomposite and PFV-graphene nanocomposite in thin film compared to the absorption spectra of PFV in thin film.

The normalized steady state emission spectra of PFV, PFV–30B nanocomposite and PFV-graphene nanocomposite in thin film (using toluene as solvent) at 297 K upon photoexcitation at 371 nm are shown in Fig. 3b. Clearly, the maximum energy position in the emission spectra of PFV is red shifted by about 8 nm in changing the medium from liquid solution (455 nm) to solid film (463 nm). This seemingly indicates that the first excited singlet state of the polymer is more stabilized in thin film due to greater interactions among the closely packed polymer chains than that in solution. Again, the emission spectra of PFV and PFV–30B nanocomposite in thin film are nearly identical with peak energy positions at 463 nm and 517 nm, though the latter spectra are slightly weaker in intensity on the red side of the spectra compared to the former spectra. Also, a vibrational peak at 424 nm is observed in the emission spectra of PFV–30B nanocomposite in thin film, which is weakly present (shoulder type) in the emission spectra of the polymer in thin film. As a result, the contribution of blue color component in the overall emission spectra is slightly more for PFV–30B nanocomposite in thin film than that for PFV in thin film. Interestingly, the emission spectra of PFV–graphene nanocomposite in thin film, with peak energy positions at 387 nm, 424 nm, 448 nm and 517 nm, are largely blue shifted compared to the emission spectra of PFV in thin film. A close look reveals that the emission maximum at 463 nm for PFV in thin film is blue shifted to 448 nm (by about 15 nm) for PFV–graphene nanocomposite in thin film. Also, the latter emission spectra show two prominent vibrational peaks at 387 and 424 nm, which are weakly present in the former ones. However, the vibrational peak position at 517 nm remains unchanged in both the spectra. Thus, the contribution of blue color component in the overall emission spectra is much higher for PFV–graphene nanocomposite in thin film than that for PFV in thin film.

It has been already reported by several authors that the incorporation of nanoparticles in the polymer chains in thin film causes a blue shift in the emission spectra of the polymer [14–16]. A blue shift in the emission spectra of a conjugated polymer is commonly associated with changes in the conjugation length. Upon incorporation of nanoparticles, bonds between a polymer chain and the nanoparticle surface may be formed. This may alter the electronic configuration in the polymer chain (*s*-*p*-hybridization occurs and the overlapping of π-orbitals decreases), thereby decreasing the conjugation length [20]. The decrease in the conjugation length may be responsible for the observed blue shift in the emission spectra. There may be another reason for the observed blue shift in the emission spectra of PFV in thin film in presence of nanoparticles in terms of the electric field produced by excess electrons on the nanoparticle surfaces [21]. The surface of the nanoparticles is a strong perturbation of the lattice and may possess a high concentration of defect levels. Upon photoexcitation, electrons from the singlet excitons of the polymer chain may populate the defect levels, thus creating an electric field outside the nanoparticles. This will raise the energy of the lowest singlet exciton state causing the observed blue shift in the emission spectra of PFV in thin film in presence of 30B nanoclay and graphene.

Steady-state emission spectra in powder form. The normalized steady-state emission spectra of PFV, PFV–30B nanocomposite and PFV–graphene nanocomposite in powder form are shown in Fig. 3c. The emission spectra of the polymer in powder form remain nearly the same compared to the spectra in thin film (with peaks at 424 nm, 463 nm and 517 nm), apart from the fact that the former spectra show enhanced intensity at 424 nm compared to that in the spectra in thin film. When the polymer is doped with 30B nanoparticles, the emission maximum is blue shifted from 463 nm to 451 nm (by about 12 nm). However, the vibrational peak position at 424 nm remains unchanged, while the shoulder at 517 nm gets reduced in intensity. When the polymer is doped with graphene nanoparticles, the emission maximum is further blue shifted from 463 nm to 447 nm (by about 16 nm). Again, the vibrational peak position at 424 nm is not affected, while the shoulder at 517 nm becomes very weak in intensity. Thus, the contribution of blue color component in the overall emission spectra is higher for

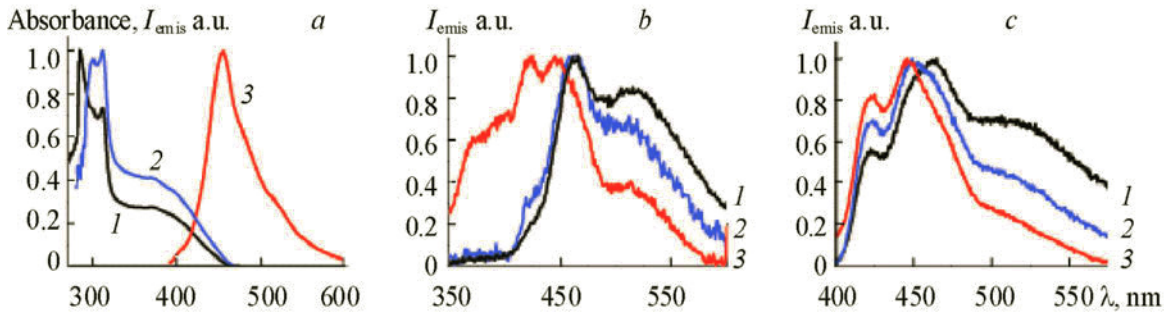

Fig. 3. (a) Normalized steady state absorption in toluene solution with OD = 0.7 at 284 nm (1) and in thin film using toluene as solvent with OD = 0.3 at 311 nm (2), as well as fluorescence emission spectra (λ_{exc} = 371 nm, in toluene solution) of PFV (0.2 mg/ml for solution and 2 mg/ml for thin film) at 297 K (3); (b) Normalized steady state fluorescence emission spectra of PFV in thin film (1), PFV–30B nanocomposite in thin film (2) and PFV–graphene nanocomposite in thin film (3) (λ_{exc} = 371 nm, using toluene as solvent) at 297 K; (c) Normalized steady-state fluorescence emission spectra of PFV in powder form (1), PFV–30B nanocomposite in powder form (2) and PFV–graphene nanocomposite in powder form (3) (λ_{exc} = 371 nm) at 297 K.

PFV–30B nanocomposite in powder form and much higher for PFV–graphene nanocomposite in powder form than that for the parent polymer in powder form. The observed blue shift in the emission spectra of PFV in powder form in presence of 30B nanoclay and graphene may be due to the changes in the conjugation length of the polymer chain as well as the electric field produced by excess electrons on the nanoparticle surface (vide supra).

Time-resolved measurements in solution. Figure 4a shows the normalized fluorescence decay curve of PFV in toluene solution at 297 K. The fluorescence lifetime values of PFV, PFV–30B nanocomposite and PFV–graphene nanocomposite in toluene solution at 297 K are given in Table 1. All the lifetimes are measured by monitoring the decay at an emission wavelength of 455 nm upon photoexcitation at 405 nm. The fluorescence decay curve of PFV in toluene solution obeys a three-exponential fit with lifetime values 0.5 ns, 1.1 ns, and 3.7 ns and associated fractional contributions are 0.19, 0.50, and 0.31, respectively. The three lifetime components may be due to the presence of shallow (1.1 ns) and deep (3.7 ns) traps along the polymer chain (the prompt fluorescence lifetime being 0.5 ns). The average lifetime of PFV in toluene solution is 1.8 ns (Table 1). No significant changes are observed in the lifetime values of PFV–30B nanocomposite and PFV–graphene nanocomposite in toluene solution compared to those of PFV in toluene solution. Again, this is expected as the interactions between the parent polymer PFV and doped nanoparticles (30B or grapheme) are insignificant in solution phase for the reason already mentioned.

Time-resolved measurements in thin film. Figure 4b shows the normalized fluorescence decay curve of PFV in thin film (using toluene as solvent) at 297 K by monitoring the emission at 463 nm upon photoexcitation at 405 nm. The fluorescence decay curve obeys a three-exponential fit with lifetime values 0.1 ns, 0.8 ns, and 5.1 ns and associated fractional contributions are 0.17, 0.30, and 0.53, respectively (Table 1). Thus, the lifetimes of the two short-lived components are further reduced (from 0.5 ns to 0.1 ns and from 1.1 ns to 0.8 ns), while the lifetime of the long-lived component is further enhanced (from 3.7 ns to 5.1 ns) in changing the medium from solution to thin film. Moreover, the major fractional contribution (about 50%) in the emission changes from the short-lived component of lifetime value 1.1 ns in solution to the long-lived component of lifetime value 5.1 ns in thin film. Consequently, the average lifetime of the polymer increases from 1.8 ns in solution to 3 ns in thin film. This may be ascribed to be due to the fact that the first excited singlet state of the polymer is more stabilized in thin film due to greater interactions among the closely packed polymer chains than that in solution as observed in the steady state emission measurements (vide supra). No significant changes are observed in the lifetime values of PFV–30B nanocomposite in thin film compared to those of PFV in thin film. However, incorporation of graphene nanopar ticles in the polymer chain in thin film enhances the lifetimes of both the short-lived components to some extent(from 0.1 ns to 0.2 ns and from 0.8 ns to 1.3 ns) and that of the long-lived component to a large extent (from 5.1 ns to 9.1 ns) compared to PFV only in thin film. Most interestingly, incorporation of graphene nanoparticles in the polymer chain in thin film makes the long-lived component (9.1 ns) the most contributing one with a fractional contribution of 87% in the emission. As a result, the average lifetime of PFV–graphene nanocomposite in thin film becomes much higher (8.1 ns) compared to that for PFV only

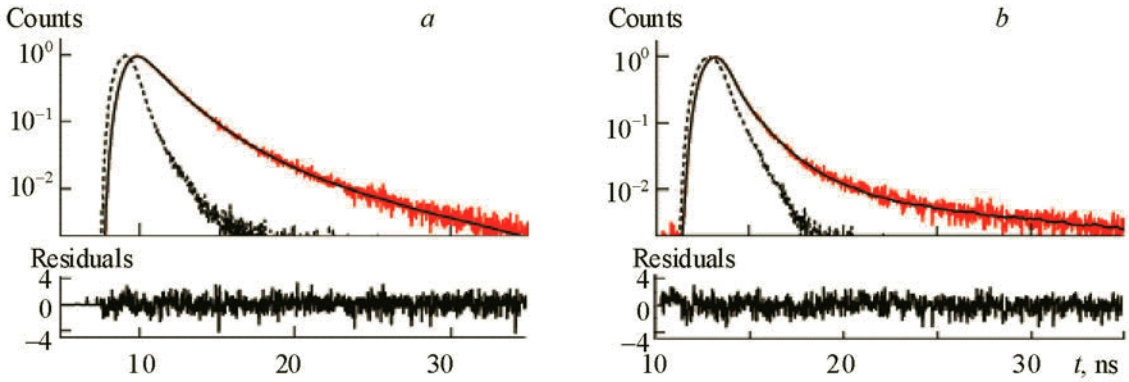

Fig. 4. Normalized fluorescence decay curve of PFV (λ_{exc} = 405 nm) at 297 K in toluene solution at λ_{em} = 455 nm (a); thin film (using toluene as solvent) at an emission wavelength of 463 nm (b). Solid black line: fitted decay curve; solid red line: original decay curve; dashed line: instrument response profile. Lower panels show the residuals for fitting.

TABLE 1. Fluorescence Lifetime Values of PFV, PFV–30B Nanocomposite and PFV-Graphene Nanocomposite in Toluene Solution (Monitored at 455 nm) as Well as Thin Film (Monitored at 463 nm, Using Toluene as Solvent) at 297 K (λ_{exc} = 405 nm)

Sample	[a]τ_1, ns	[a]τ_2, ns	[a]τ_3, ns	a_1, %	a_2, %	a_3, %	χ^2	DW	[b]f_1	[b]f_2	[b]f_3	[c]$\langle\tau\rangle$, ns
PFV (solution)	0.5	1.1	3.7	41.9	49.0	9.1	1.01	1.85	0.19	0.50	0.31	1.8
PFV–30B (solution)	0.5	1.1	3.7	46.5	45.0	8.5	1.02	1.91	0.22	0.47	0.31	1.8
PFV–graphene (solution)	0.4	1.2	3.5	41.7	47.3	11.0	1.11	1.86	0.15	0.51	0.34	1.9
PFV (film)	0.1	0.8	5.1	78.2	17.1	4.7	1.12	1.81	0.17	0.30	0.53	3.0
PFV–30B (film)	0.1	0.8	5.1	78.2	17.1	4.7	1.13	1.81	0.17	0.30	0.53	3.0
PFV–graphene (film)	0.2	1.3	9.1	45.6	24.9	29.5	1.14	1.74	0.03	0.10	0.87	8.1

[a]Triple exponential fit used: $c + a_1 \exp(-t/\tau_1) + a_2 \exp(-t/\tau_2) + a_3 \exp(-t/\tau_3)$.
[b]Fractional contribution of each decay component is $f_i = a_i\tau_i/(\Sigma a_j\tau_j)$, where a_j is the pre-exponential coefficient of the jth decay component.
[c]Average fluorescence lifetime is $\langle\tau\rangle = \Sigma f_i\tau_i$ (i = 1, 2, 3).

in thin film (3 ns). This seemingly indicates that the deep trap sites, which might be responsible for the long-lived component (vide supra), move further deeper in the polymer chain in presence of the doped graphene nanoparticles in thin film. It is noteworthy that this is the first attempt, to the best of our knowledge, to understand the basic optical properties of polymer nanocomposites by means of time-resolved data (of the order of ps-ns). Obviously, more time-resolved measurements are needed on several polymer nanocomposites (with different polymers as well as different nanoparticles) to see the generic nature of the fluorescence lifetime components and their relative contributions so as to give proper explanations based on a suitable model. These works are now under progress in our laboratory and will be reported later.

Conclusions. Optical properties of the fluorescent conjugated polymer PFV are investigated in liquid medium (using toluene as solvent) and solid phase (spin coated thin film as well as powder form) by using steady state and time-resolved spectroscopic techniques. Significant red shift is observed in the fluorescence emission of PFV in solid phase compared to that in liquid medium. Polymer nanocomposites are prepared by doping PFV with 30B nanoclay and graphene nanoparticles. Material characterizations of the polymer and its nanocomposites are carried out by FTIR and TGA techniques. Appreciable color tuning in the emission of PFV in the blue side of the spectra is achieved by doping the polymer with 30B nanoclay and especially graphene in solid phase (greater blue shift in powder form than in thin film). Moreover, the average fluorescence

lifetime increases by about three times in PFV–graphene nanocomposite in thin film relative to that of PFV only in thin film. These investigations are extremely important in view of the potential applications of these novel polymer nanocomposites in the fabrication of polymer optoelectronic devices.

Acknowledgments. Subrata Sinha thanks Sukhendu Nath (Radiation and Photochemistry Division, Bhabha Atomic Research Centre, Trombay, Mumbai, India) for fluorescence lifetime measurements.

REFERENCES

1. C. K. Chiang, C. R. Fincher, Jr, Y. W. Park, A. J. Heeger, H. Shirakawa, E. J. Louis, S. C. Gau, and A. G. MacDiarmid, *Phys. Rev. Lett.*, **39**, 1098–1101 (1977).
2. J. H. Burroughes, D. D. C. Bradley, A. R. Brown, R. N. Marks, K. Mackay, R. H. Friend, P. L. Burns, and A. B. Holmes, *Nature*, **347**, 539–541 (1990).
3. S. Mazumdar, *Science*, **288**, 630–631 (2000).
4. H. Althues, P. Simon, and S. Kaskel, *J. Mater. Chem.*, **17**, 758–768 (2007).
5. X. Hu, H. An, Z. Li, Y. Geng, L. Li, and C. Yang, *Macromolecules*, **42**, 3215–3218 (2009).
6. S. Barrau, C. Vanmansart, M. Moreau, A. Addad, G. Stoclet, J. Lefebvre, and R. Seguela, *Macromolecules*, **44**, 6496–6502 (2011).
7. N. K. Singh, S. K. Singh, D. Dash, P. Ganugunta, M. Misra, and P. Maiti, *J. Phys. Chem. C*, **117**, 10163–10174 (2013).
8. P. Pan, B. Zhu, T. Dong, and Y. Inoue, *J. Polym. Sci. Part B: Polym. Phys.*, **46**, 2222–2233 (2008).
9. P. C. LeBaron, Z. Wang, and T. J. Pinnavaia, *Appl. Clay Sci.*, **15**, 11–29 (1999).
10. N. K. Singh, B. D. Purkayastha, J. K. Roy, R. M. Banik, M. Yashpal, G. Singh, S. Malik, and P. Maiti, *Appl. Mater. Interfaces*, **2**, 69–81 (2010).
11. K. K. Jana, B. Ray, D. K. Avasthi, and P. Maiti, *J. Mater. Chem.*, **22**, 3955–3964 (2012).
12. H. Kim, A. A. Abdala, and C. W. Macosko, *Macromolecules*, **43**, 6515–6530 (2010).
13. S. A. Jenekhe and J. A. Osaheni, *Chem. Mater.*, **6**, 1906–1909 (1994).
14. L. Bakueva, S. Musikhin, E. H. Sargent, and A. Shik, *Surface Sci.*, 532–535, 1051–1055 (2003).
15. S. H. Yang, T. P. Nguyen, P. Le Rendu, and C. S. Hsu, *Thin Solid Films*, **471**, 230–235 (2005).
16. N. N. Dinh, L. H. Chi, T. T. C. Thuy, D. V. Thanh, and T. P. Nguyen, *J. Korean Phys. Soc.*, **53**, 802–805 (2008).
17. F. Bonaccorso, Z. Sun, T. Hasan, and A. C. Ferrari, *Nature Photonics*, **4**, 611–622 (2010).
18. K. S. Novoselov, A. K. Geim, S. V. Morozov, D. Jiang, Y. Zhang, S. V. Dubonos, I. V. Grigorieva, and A. A. Firsov, *Science*, **306**, 666–669 (2004).
19. K. S. Novoselov, D. Jiang, F. Schedin, T. J. Booth, V. V. Khotkevich, S. V. Morozov, and A. K. Geim, *Proc. Natl. Acad. Sci. USA*, **102**, 10451–10453 (2005).
20. M. Dekker, *Handbook of Conjugating Polymers*, New York (1998).
21. S. Musikhin, L. Bakueva, E. H. Sargent, and A. Shik, *J. Appl. Phys.*, **91**, 6679–6683 (2002).